

Alteration of fluid properties during the initial operation of a geothermal plant: results from in situ measurements in Groß Schönebeck

Elvira Feldbusch · Simona Regensburg · Jonathan Banks · Harald Milsch · Ali Saadat

Received: 15 October 2012 / Accepted: 9 March 2013 / Published online: 4 April 2013
© Springer-Verlag Berlin Heidelberg 2013

Abstract Recently, the thermal fluid loop has been established and continuously operated for 7 days at the geothermal in situ laboratory in Groß Schönebeck (North German Basin). During this initial phase of fluid production, the fluid temperature, measured at the surface, continuously increased until a stable value of about 98 °C was established. Fluid physicochemical properties (pH, redox, density, temperature, and pressure) were measured online and in situ with a newly developed fluid monitoring system (FluMo). Additionally, fluid samples have been collected at various temperatures (in 5–10 °C steps) directly at the production well at about 10 bar pressure. From the pressurized sampling tool, the fluid was directly transferred into a heated autoclave, which allowed filtration (0.2 µm) in the absence of oxygen. Physicochemical parameters [pH, redox, electric conductivity, total dissolved solids (TDS)] as well as acid capacity ($K_{S\ 4.3}$) of these samples have been measured onsite at atmospheric conditions. Concentrations of anions, total organic carbon, and metals were analyzed later in the laboratory. Both, measurements in collected samples or in situ (FluMo) analysis of most the parameters density, electric conductivity, or TDS indicated relatively constant values over the whole production time (1.17–1.18 g · cm⁻³, 215–221 mS · cm⁻¹, 241–260 g · L⁻¹, respectively). Good correlation was also found for pH values (pH = 6.6–6.9), whereas the redox values varied between –1 and 46 mV when determined at 25 °C and decreased strongly when measured in situ with increasing temperature (–110 mV at 90 °C). The elemental

composition of collected samples remained also relatively constant for most compounds and was clearly higher as compared with samples collected in 2011. Results of this study demonstrate that realistic, comprehensive, and time-resolved physicochemical data can be obtained by FluMo. These detailed data sets can be crucial to understand the complex geochemical processes in a thermal water loop and eventually to take required measures on time.

Keywords Geothermal energy · Geothermal fluid · Geochemical monitoring · Physicochemical properties of fluids · North German Basin · Rotliegend · In situ laboratory Groß Schönebeck

Introduction

The demand of energy increases worldwide boosting also the development of environmentally friendly technologies such as geothermal energy (Eggeling et al. 2011). This energy resource is nearly ubiquitously available, emits—as compared with fossil fuels—hardly CO₂, and can be used for both heating and generation of electricity (Bührke and Wengenmayr 2012).

However, the production of electricity especially requires the geothermal fluid to be of sufficiently high temperature (>100 °C) and to derive from a geological reservoir that allows fluid production of high flow rate (>100 m³ · h⁻¹) (Huenges 2010). No high-enthalpy geothermal steam reservoirs exist in central Europe and for the exploitation of low-enthalpy systems the construction of binary cycle power plants are required (Tenzer et al. 2010). In Germany, only few geological areas are suitable for the installation of geothermal power plants. The North German Basin represents a sedimentary basin that contains several

E. Feldbusch · S. Regensburg (✉) · J. Banks · H. Milsch · A. Saadat
GFZ German Research Centre for Geosciences,
Telegrafenberg, 14473 Potsdam, Germany
e-mail: regens@gfz-potsdam.de

sandstone layers (such as Triassic Buntsandstein or Permian Rotliegend) that are marked by sufficient high permeability required for high fluid production rates (Scheck and Bayer 1999; Friberg et al. 2000; Magri et al. 2005).

These formation fluids are typically marked by high salinity of several hundred grams per liter, representing a challenge for power plant operation due to potential mineral precipitation or material corrosion within the geothermal fluid loop (Regenspurg et al. 2010; Norden et al. 2008).

At the in situ geothermal research facility Groß Schönebeck (GrSk), located in the North German Basin (Brandenburg, Germany; 52.90°N, 13.58°E), processes linked to exploitation of geothermal energy and electricity production are intensely investigated and new technologies developed (Huenges et al. 2006). The geothermal fluid loop consists of a well doublet for fluid production and injection, respectively, drilled to a depth of 4400 m encountering Permian (Rotliegend) vulcanite and sandstone layers. Reservoir hydrostatic pressure is 44 MPa and the fluid temperature is about 150 °C at depth (Huenges 2004; Blöcher et al. 2008). Above ground, the accumulated fluid would be degassed and after heat transfer to an organic medium via a heat exchanger, the cooled fluid would be re-injected into the reservoir via the injection well. However, so far, the fluid loop is not yet connected to the heat exchanger and only production and injection tests have been performed. During these tests fluid investigations were possible and the results of these newly developed methods are presented in this paper.

The composition of the Groß Schönebeck reservoir fluid has been known from previous studies (Regenspurg et al. 2010). It is characterized as Na–Ca–Cl type water, which has been evolved by numerous processes of evaporation, dissolution, and continuous interactions with reservoir rocks over millions of years (Regenspurg et al. 2010; Schmidt Mumm and Wolfgramm 2002, 2004).

In general, the content of dissolved species in these old sedimentary basin formations can be described as highly diverse and complex. With up to 330 g · L⁻¹ total dissolved solids (TDS) and relatively low acidity (pH = 5–7), these fluids contain high concentrations of alkaline-, alkaline earth, and heavy metals with chloride, sulfate, carbonate, and low-molecular organic acids as counter ions and additional neutral organic compounds (Lüders et al. 2010, 2005; Tesmer et al. 2007).

The GrSk thermal fluid also contains a high volume of dissolved gases (volume ratio of liquid:gas is about 1:1 at reservoir conditions), which are mainly composed of nitrogen (N₂; 84–90 Vol.%) and methane (CH₄; 10–16 Vol.%) with minor concentrations of CO₂, H₂, He, Ethane and Kr, Propane, n-Buthane, and i-Buthane released at the surface due to pressure drop into the atmosphere.

Only CO₂ would remain in the solution because the pressure at the Groß Schönebeck facility is kept at 10–15 bar to prevent CO₂ degassing and the associated pH increase, and potential carbonate precipitation.

Changes of the thermodynamic equilibrium, for example, by decreasing temperature and pressure in the above-ground installations of the closed loop of a geothermal plant can affect the chemical composition of the thermal water (Regenspurg et al. 2010). Consequently, many alkaline earth and heavy metals of the GrSk fluid might precipitate as hardly soluble minerals. These so-called “scalings” are specifically undesirable in geothermal power plants because they might clog the pipes of the installation or the pores of the reservoir, thus causing major failures of the plant. For example, dissolved sulfate of the reservoir fluid could precipitate upon cooling as barite (BaSO₄), coelestine (SrSO₄), or gypsum (CaSO₄ · 2 H₂O) as it has been described in numerous studies (Kühn 1997).

In order to understand, predict, and eventually prevent these reactions, a detailed monitoring of fluid physico-chemical parameters and of the chemical composition is required which should be able to measure both, at various locations within a geothermal facility, and continuously over time during the operation of the plant.

Typically, these parameters are determined after sampling of fluid and subsequent degassing and cooling, thereby transformations of the solution composition are unavoidable, due to the change of thermodynamic conditions and consequent chemical reactions (Buffle and Horvai 2000). Although these methods are generally approved and frequently applied for exploration of geothermal sites (Gultekin et al. 2011; Liu et al. 2012), they are insufficient for determination of physicochemical processes during operation of a geothermal plant. In situ measurements at given temperatures, pressures, and salinities of most geothermal waters (such as GrSk) are not possible with commercially available probes (e.g. pH, redox, electric conductivity).

In a new study, high-salinity resistant electrodes and measurement devices have been combined (Milsch et al. 2013) with a fluid monitoring device (“FluMo”), that could be connected to several locations in the above-ground installations of GrSk (e.g. before and after the filters and degasser) allowing in situ measurements and data storage of temperature, pressure, fluid flow, density, oxygen, redox- and pH value.

This paper shows first results of online measurements performed with FluMo and compares and discusses the obtained data with chemical and physicochemical analysis of samples collected simultaneously at the same site. Since the fluid loop in GrSk was to this day still in test phase (continuous operation of the pumps for few hours up to 7 days), the conditions represent a unique chance for

observing changes of the mentioned parameters during heating and cooling of the fluid in the initial pumping phase.

Materials and methods

Fluid production tests at the geothermal research platform Groß Schönebeck

At the geothermal research facility in Groß Schönebeck, the fluid loop was established in March 2011. Before connection to the power plant several fluid production and injection (circulation) tests have been carried out between April 2011 and May 2012 to optimize the installation set-up. These tests lasted between few hours and 1 week allowing sampling of geothermal fluid directly from the production well head. During the last and longest test phase (7 days in April 2012), it was also possible for the first time to connect the fluid monitoring system “FluMo” to the loop and obtain in situ data of several physicochemical parameters (pH, redox, density).

This study compares results from samples collected during a test period in August 2011 and the 1-week test period in April 2012. Throughout both periods, fluid temperature at the well head slowly increased with time up to maximum values of about 100 °C.

During the first sampling periods in August 2011, the production was non-continuous (pumps stopped after few hours), whereas during the last production test (started at the 17th of April 2012) a continuous production was achieved. In the beginning of this test, the production rate was about $80 \text{ m}^3 \cdot \text{h}^{-1}$ and decreased during the first day to about 20, and to $15 \text{ m}^3 \cdot \text{h}^{-1}$ on the next day. Afterwards, the flow rate remained constant until the end of the experiment on the 24th of April 2012. The initial temperature was about 70 °C at the pump and 20 °C at the surface. Upon reaching about 100 °C on the surface and 130 °C at the pump (9th of April 2012), the fluid temperature remained constant until the end of experiment. The pressure in the above-ground installations of the plant ranged between 8 and 12 bars.

During the shorter non-continuous production tests in August/September 2011, operating conditions were similar, with flow rates of at least $20 \text{ m}^3 \cdot \text{h}^{-1}$.

Fluid sampling and preparation

Fluid samples have been collected at various temperatures (in 5–10 °C steps) during fluid production directly at the production well at about 10 bar pressure with a BIAR—inline sampling system. This device consists of a portable BIAR—COLUMBIA sampler and a corresponding BIAR

bajonet (D’EMPLOI) adapter, connected to the pipe. Before sampling, 1–2 L of fluid was discarded and afterwards the pressurized and nitrogen flushed. Columbia sampler was connected to the pipe, allowing to sample about 50 mL fresh fluid. The sampler was directly transferred into a heated autoclave that had been flushed with nitrogen and pressurized before (Fig. 1). The pressure in the autoclave was about 2 bar less than in the sampler allowing the fluid to flow directly into the autoclave. By slow pressure release, fluid would pass first from the autoclave through a filter (0.2 μm) and (by needle injection through a septum) into a previously nitrogen-flushed and ice-cooled bottle (Fig. 1). The septum bottle was attached to a bubble counter for pressure stabilization. The sample collected in the septum bottle was immediately placed into a refrigerator until anion analysis (see “sample analysis”).

The samples for metal analysis were directly added from the autoclave into a 15 mL tube containing 200 μL of 6 M HNO_3 . For TOC determination non-filtered original sample were injected into septum bottles. All samples were stored until analysis at 4 °C.

Immediately after sampling, a third subsample (20 mL) was removed from the autoclave to determine directly physicochemical parameters at ambient pressure and temperature (25 °C).

Sample analysis

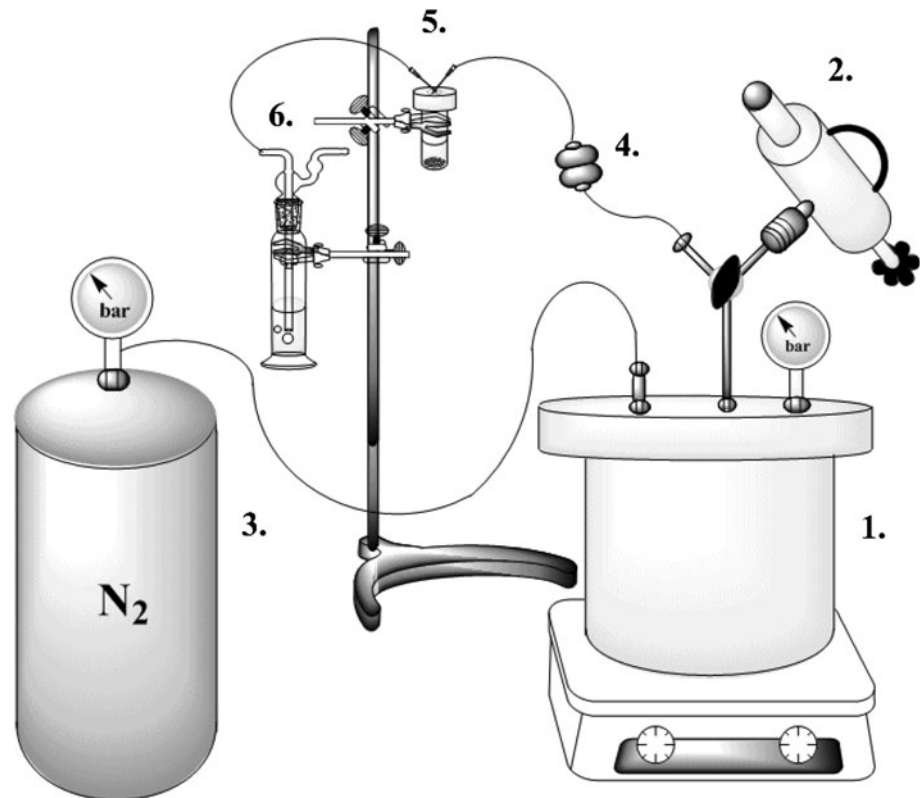
All electrodes and methods applied have been specifically developed for use in highly saline solutions.

Determination of bicarbonate (HCO_3^-) in thermal waters is impeded by the presence of further salts of weaker acids (borates, silicates, acetates and formates) (Bukatsch 1938). Therefore, the acid capacity ($K_{S\ 4.3}$) of the fluid was determined titrimetrically with 0.1 M HCl and methyl orange (Hall and Niessner 2010).

The redox value was measured with a combined platinum electrode with an Ag/AgCl reference in advanced gel electrolyte system (a polymer-based gel with 3 M KCl providing constant ionic strength). For determining the pH-value, a glass electrode with Ag/AgCl reference system and a similar advanced gel KCl system (pressurized to 6 bar) were used. Both, redox and pH electrode, have been designed for application at temperatures up to 100 °C [Endress + Hauser, types: CPS71D-7BP21 (pH) and CPS12D (redox)].

Since the pH value, measured by electrodes in highly saline solutions, shifts towards lower values, a pH correction factor must be determined for each electrode (Altmaier et al. 2003). For this purpose, several pH standards with similar ionic strength as the fluid ($I = 3.6 \text{ mol} \cdot \text{L}^{-1}$, adjusted with NaCl and CaCl_2) were prepared with HCl or NaOH. An experimental pH_{exp} was measured in these

Fig. 1 Sampling device: 1 autoclave on heating plate with heat jacket, magnetic stirrer and manometer; 2 BIAR-Colombia sampling bottle (pressurized); 3 nitrogen bottle (200 bar) for pressurizing and flushing the autoclave and septum bottle; 4 filter unit (0.2 μm membrane filter); 5 sample bottle with septum lid; 6 bubble counter



standards. By applying the formula $\text{pH}_{\text{exp}} = \text{pH} - A$ the pH shift A was calculated. For the used electrodes, correction factors +1.1 (at 25 °C) for onsite measurements and +1.2 (at 25 °C) for FluMo measurements were determined, which is very typical for solutions of high salinity (Almaier et al. 2003).

For temperature correction of in situ determined pH, we used the following calculation, where $A_{T=0}$ is equivalent to pH-shift at 0 °C:

$$\begin{aligned} \text{pH} &= \text{pH}_{\text{exp}} + A(T) \\ &= \text{pH}_{\text{exp}} + \Delta A / \Delta T \cdot T + A_{T=0} \\ &= \text{pH}_{\text{exp}} + 7 \times 10^{-3} \cdot T + 1.05 \end{aligned}$$

The TDS were determined by weighing the dried (130 °C) filtrate of 2 mL fluid (residue of evaporation). The electric conductivity was measured with a four-electrode graphite conductivity probe (measuring range: 0.01–2000 $\text{mS} \cdot \text{cm}^{-1} \pm 0.5\%$ of measured value and temperature accuracy of 0.2 °C). Fluid density was determined with a handset density meter (Anton Paar, measurement principle by bending vibration; allowing an accuracy of 0.001 $\text{g} \cdot \text{cm}^{-3}$ and 0.2 °C, respectively).

Metals were analyzed by inductive coupled plasma mass spectrometry (ICP-MS, Element2 ThermoScientific). Ammonium was measured spectro-photometrically with a Specord200 (Analytik Jena AG) and total organic carbon

(TOC) by Foss Heraeus Analysensysteme with high-temperature application (LiquiTOC). Anion compositions were measured by ion chromatography (IC; 882 COMPACT IC PLUS-Anionen-MCS, Metrohm). The corresponding detection limits and uncertainties are summarized in Table 1.

Measurements with FluMo

A detailed description of the fluid monitoring system FluMo is given by Milsch et al. (2013). Briefly, the measurement and sampling device, developed at GFZ, can be connected to different locations at the above-ground geothermal loop (e.g. in Groß Schönebeck). In a bypass system, the fluid would enter the FluMo-apparatus and pass a flow meter (Endress + Hauser) and a density meter (Anton Paar, mPDS 1100) of high accuracy ($10^{-4} \text{g} \cdot \text{cm}^{-3}$). Following that the fluid can be cooled down to a designated temperature at a heat exchanger (the device was not in use for the experiments described in this study).

In the following flow-through cell a pH glass-, as well as a redox platinum electrode with Ag/AgCl reference electrode (both of the same type as described above for lab measurements) was installed. Finally, the fluid would be cooled to below 50 °C and oxygen concentration could be measured in a third flow-through cell equipped with an oxygen electrode (Endress + Hauser, Oxymax COS22D, oxygen reduction

Table 1 Detection limits and accuracies of used analytical methods

Parameter	Analysis device	Detection limit	Accuracy (%)
Ammonium	UV/VIS	0.01 mg · L ⁻¹	10
Sodium	ICP-MS	100 mg · L ⁻¹	10
Potassium		6 mg · L ⁻¹	10
Calcium		20 mg · L ⁻¹	10
Magnesium		0.07 mg · L ⁻¹	10
Iron		0.02 mg · L ⁻¹	10
Manganese		0.05 mg · L ⁻¹	8
Aluminum		0.001 mg · L ⁻¹	12
Lithium		40 µg · L ⁻¹	8
Boron		350 µg · L ⁻¹	10
Silicon		0.5 mg · L ⁻¹	10
Chrome		0.4 µg · L ⁻¹	10
Nickel		0.9 µg · L ⁻¹	10
Copper		0.8 µg · L ⁻¹	10
Zinc		40 µg · L ⁻¹	10
Arsenic		0.5 µg · L ⁻¹	10
Strontium		1.0 mg · L ⁻¹	8
Cadmium		0.03 µg · L ⁻¹	10
Barium		150 µg · L ⁻¹	10
Mercury		0.2 µg · L ⁻¹	10
Lead		100 µg · L ⁻¹	10
Chloride	IC	2,500 mg · L ⁻¹	5
Sulfate		10 mg · L ⁻¹	5
Formate		<1 mg · L ⁻¹	5
Acetate		<1 mg · L ⁻¹	5
Fluoride		<1 mg · L ⁻¹	5
Bromide		<1 mg · L ⁻¹	5
Oxalate/ Fumarate		<1 mg · L ⁻¹	5
TOC	LiquiTOC	0.2 mg · L ⁻¹	15

cathode with Ag/AgCl anode). All parameters were automatically recorded and every second. FluMo was operated for the first time in April 2012 during the 7-day production experiment (2 h after switching on the pumps).

FluMo was connected to the above-ground installation right before fluid reinjection. This location was chosen for the first experiment because the most homogenous conditions of the fluid would be established, e.g., the fluid would be almost completely degassed (apart from CO₂ which should remain upon the given pressure in solution) and it would have passed two sets of filter bags (1–2 µm). The flow rate of the fluid circling in the FluMo system was adjusted manually to approximately 1.7 L · min⁻¹ at a pressure of 4–5.5 bar.

The pH value correction factor was also determined for the FluMo electrodes before operation at various temperatures (19–80 °C) at ambient pressure under laboratory

conditions. After operation the deviation of the correction parameter *A* was <0.05.

Results and discussion

Parameters measured with the in situ fluid monitoring system FluMo

The 7-day long-term production-injection experiment started on the 17th of April 2012. After 2 h of fluid production, FluMo was connected to the fluid loop when the temperature at the surface was already 52 °C. Data (temperature, pressure, flow rate, density, pH, redox and oxygen) were measured and recorded permanently (every second) until the end of the circulation test after 160 h. Examples of monitoring data are shown in Figs. 2, 3 and 4.

Basically, two phases can be distinguished: at the initial phase, when the temperature of the fluid was still increasing, the measured parameters were still relatively unstable. This can be expected because the thermodynamic equilibrium of the fluid was not yet established. At the first day (17th of April), the density decreased with increasing temperature from 1.1640 g · cm⁻³ (52 °C) at a rate of 10⁻⁶ g · cm⁻³ per 1 °C (Fig. 2). This temperature—density correlation is given because volume and density are inversely proportional and the change in density by temperature can be expressed as follows: $\delta_2 = \delta_1 / (1 + \gamma \cdot \Delta T)$, where δ_1 , δ_2 is the density, γ the thermal expansion coefficient and ΔT the temperature change.

Occasional variations in density correlate with temporary failures of the circulation pump in FluMo. A much stronger decrease in density (from 1.16 to 1.14 g · cm⁻³) occurred at about 6 pm indicating the arrival of either a gas bubble or an admixture of fluid of lower salinity to the formation fluid. After a few hours the density was again at the original range (1.152 g · cm⁻³ and upon reaching a fluid temperature of 79 °C on the same day, a density of 1.1502 g · cm⁻³ was measured).

During this initial phase of the experiment the pH- and redox values showed relatively strong variations that are mainly an effect of temperature (Fig. 3). The pH value decreased from 6.7 at 50 °C to 6.5 at 79 °C which can be explained by the Nernst equation stating that the activity of protons (= decrease of pH) would increase with increasing temperature. Similarly, the Nernst equation explains a decrease in redox potential with increasing temperature as found in situ, where the redox decreased from -20 to -40 mV in the same temperature range. However, several outliers in the curve suggest unstable conditions indicating also redox reactions (Fig. 3).

Both, pH- and redox values showed an abnormality at the same time (6 pm) as also observed from the strong

Fig. 2 Online data of temperature and density measured with the FluMo system in situ at the initial phase of the experiment (17 April 2012)

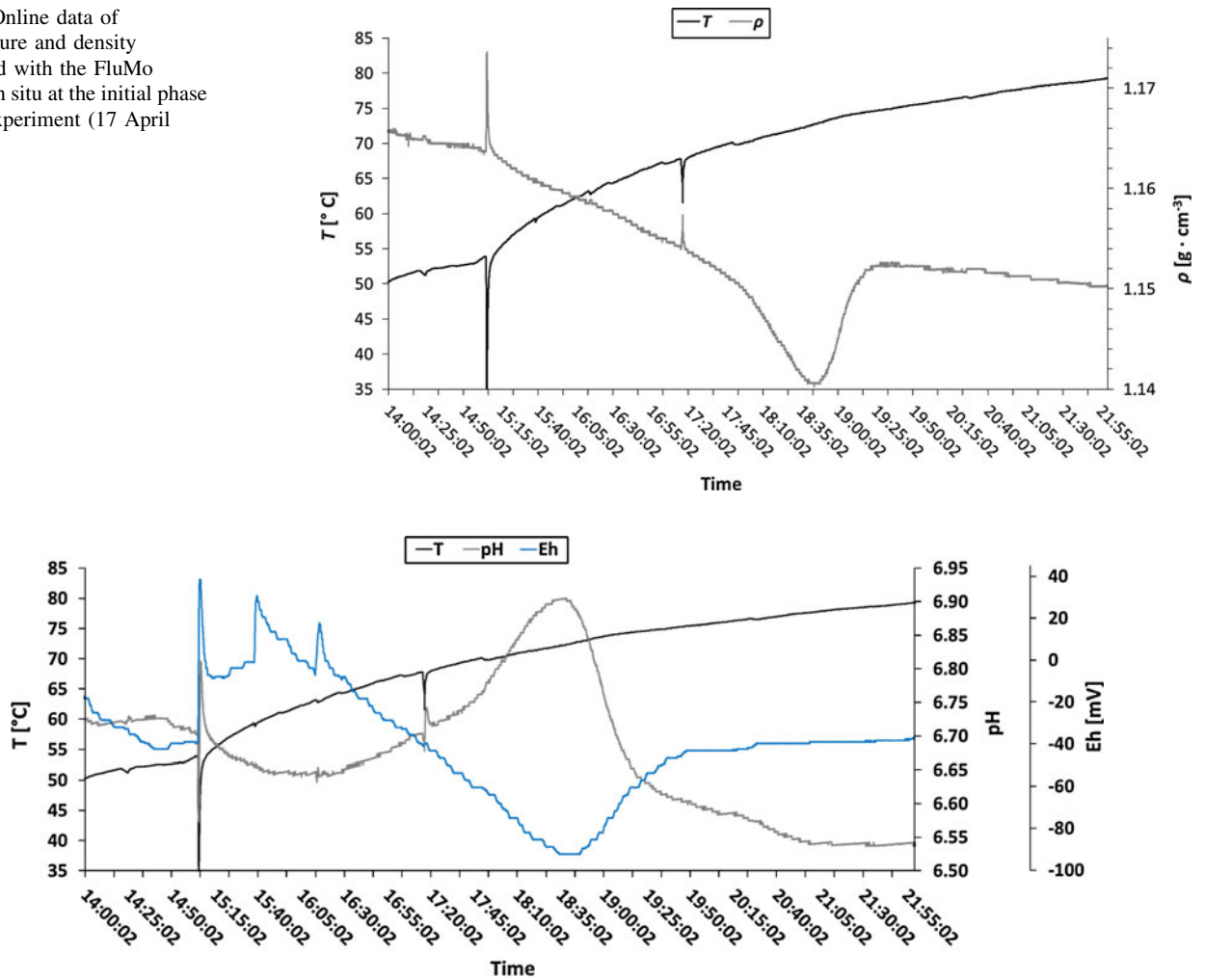


Fig. 3 Online data of temperature (black), redox (light gray) and pH value (shift-corrected; dark gray) measured with the FluMo system in situ at the initial phase of the experiment (17 April 2012)

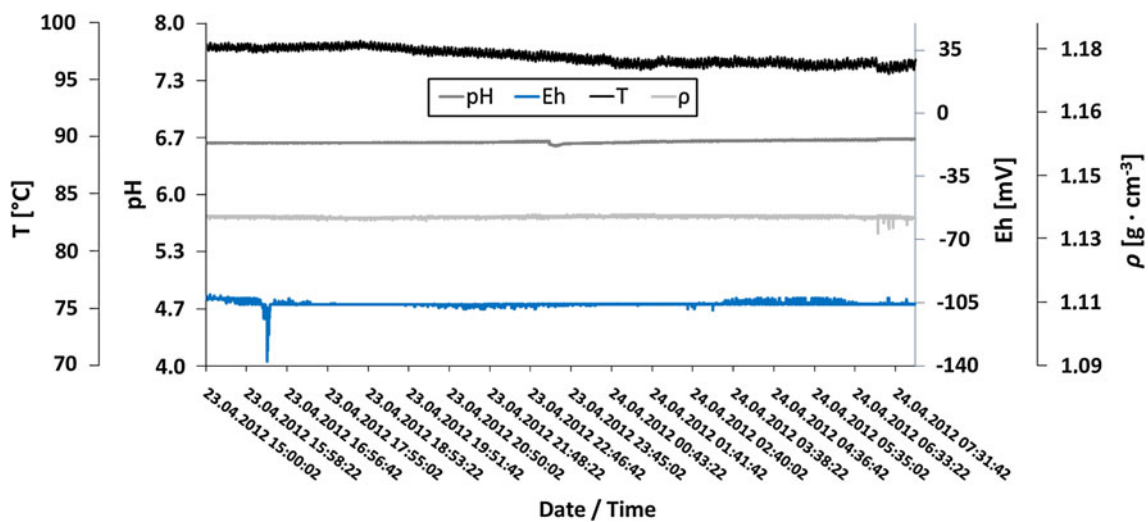
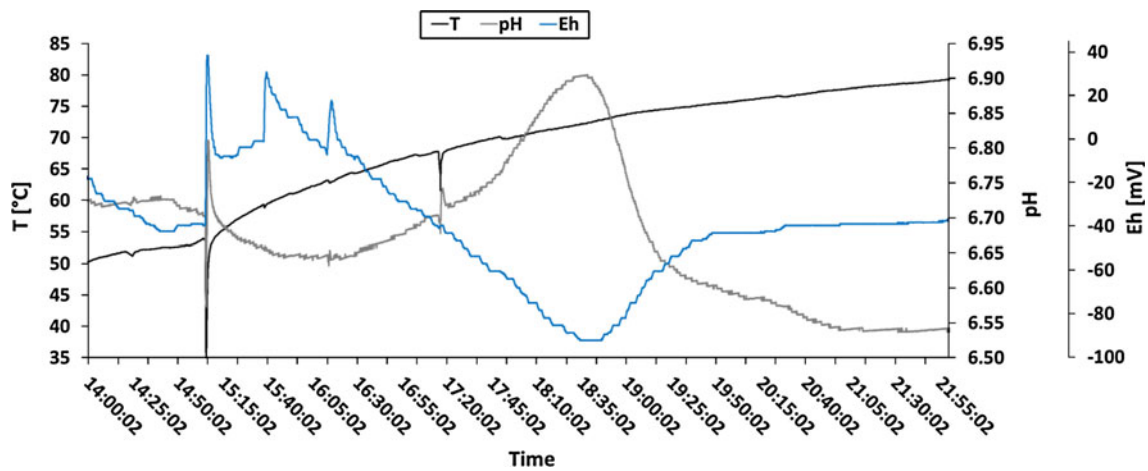


Fig. 4 Online data of temperature, density, redox, and pH measured with the FluMo system over 2 days in situ [stable phase of the experiment at constant temperature (92 ± 2 °C) in FluMo]

density change, indicating the arrival of a different water type at the sensors, rather than a gas bubble.

During the second phase of the circulation experiments (after 48 h on the 19th of April 2012), towards the end of the circulation experiment, the fluid temperature had stabilized at 98 ± 3 °C. At this temperature, no further variations in physicochemical data were observed (Fig. 4). The pH value had stabilized to about 6.6 and density to $1.132 \text{ g} \cdot \text{cm}^{-3}$. The fluid shows clearly reductive characteristic with an Eh of about -105 mV .

The oxygen content in the fluid was between 0 and $1 \text{ mg} \cdot \text{L}^{-1}$. After filter exchange (clogging of filter groups in the fluid loop over time), the oxygen increased briefly up to $7 \text{ mg} \cdot \text{L}^{-1}$. The flow rate in FluMo was at $2\text{--}4.5 \text{ L} \cdot \text{min}^{-1}$ and the internal pressure $4\text{--}5.5 \text{ bar}$.

Samples collected at the well head

Figure 5 shows the amount of accumulated fluid over time and marks the area of the two sampling periods compared in this study. During the 1-week production test in April 2012 altogether 2624 m^3 of fluid have been produced and reinjected (Fig. 5). In August 2011, during four production attempts (each about 6 h), around 1200 m^3 fluid were produced (Fig. 5).

In the following, data are mainly presented from the period in 2012 because they can be directly compared with data measured by FluMo. Moreover, it can be assumed that more reservoir-like conditions were established at this (later) time of the circulation tests.

In samples collected at the well head electric conductivity, redox, pH value, density, and TDS were determined. Results are summarized in Table 2 and shown in Figs. 6, 7 and 8.

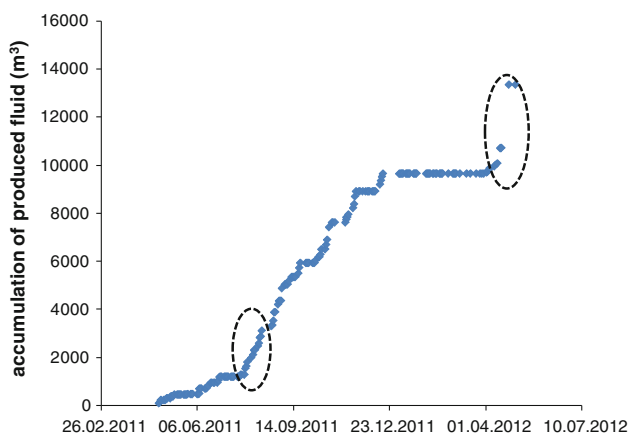


Fig. 5 Amount of accumulated produced fluid measured over time from the beginning of circulation tests. *Dashed circles* show the two sampling periods in August 2011 and in April 2012

At the beginning of the production phase, the temperature continuously increased over time. Concurrently, density and TDS varied strongly, indicating unstable conditions and potentially sporadic mixing of different fluid layers (Fig. 6). After 1–2 days, density stabilized at about $1.179 \text{ g} \cdot \text{cm}^{-3}$ and TDS in the range of 240 and $270 \text{ g} \cdot \text{L}^{-1}$, respectively (Fig. 6).

Acidity of the fluid remained constantly relatively neutral throughout the experiment (at pH 6.6–6.8) (Fig. 7). Similarly, acid capacity of the thermal water remained stable at ambient conditions ($K_{S\ 3.4} = 1.8 \pm 0.1 \text{ mol} \cdot \text{L}^{-1}$) implying that the acid–base equilibrium remained constant during the entire operation. In contrast, relatively strong fluctuations have been observed for the redox potential throughout the production test ranging at slightly oxidizing values (at ambient conditions) between -2 and $+40 \text{ mV}$ (Fig. 7).

While the values for density and TDS strongly correlate with each other, electric conductivity showed some deviations (Fig. 8). The comparison of TOC which contains normally charged and uncharged components with electric conductivity (just charged components) and TDS (charged and uncharged) showed that both, TDS and TOC increased over time, whereas electrical conductivity remained constant indicating that the content of non-charged components (such as organic molecules) grows over time and temperature.

The major components of the thermal water are dissolved sodium (Na), calcium (Ca), and chloride (Cl) which vary slightly during operation (Ca from 1.2 to 1.4 M; Cl from 4.1 to 4.7 M and Na from 1.8 to 1.7 M) (Fig. 9). The total molar equivalent of chloride correlates very well with the molar sum of Na, Ca, K, Sr and Li.

The concentration of potentially oversaturated phases such as barium, iron, or lead-species remained relatively constant throughout the fluid production, indicating that the fluid is already in equilibrium with respect to these phases (Fig. 10). An exception is the concentration drop of many compounds at 75.1 °C (17th of April; Fig. 10). This sudden concentration change occurs at the same time (6 pm) as the observed changes in pH, redox, and density as described earlier.

In this group of components, manganese dominates with $3.7\text{--}4.1 \text{ mM}$, whereas silica, iron, and zinc are in the same concentration range. Silica concentration varies little ($1.2\text{--}1.5 \text{ mM}$). Iron and zinc concentration range between 1.0 and 1.4 mM , lead between 0.5 and 0.8 mM , and barium between 0.3 and 0.5 mM (Fig. 10).

The comparison between analytical results of samples collected during the production test from August 2011 with data from April 2012 revealed little differences for calcium and chloride. In April 2012 concentrations were generally higher, e.g. the calcium content had increased for 0.1 M

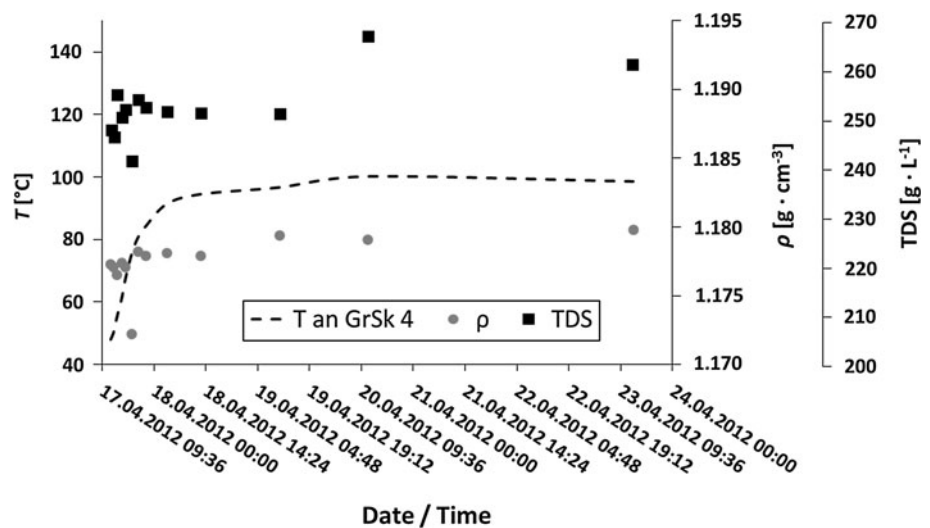
Table 2 Onsite determined parameters of collected thermal water samples during continuous operation (April 2012)

Sampling date (time)	T (°C) wellhead	Accumualed produced fluid (m ³)	σ (mS · cm ⁻¹)	Eh (mV)	pH	ρ (g · ml ⁻¹)	TDS (g · L ⁻¹)
17.04.2012 (12:00)	48.0	9.9	216 (25.2 °C)	42 (25.7 °C)	6.63 (23.3 °C)	1.1773 (23.9 °C)	248.1
17.04.2012 (12:50)	50.5	37.5	215 (26.1 °C)	23 (26.4 °C)	6.64 (26.1 °C)	1.1771 (23.7 °C)	246.7
17.04.2012 (13:40)	54.9	56.9	216 (26.5 °C)	30 (26.4 °C)	6.70 (24.1 °C)	1.1765 (23.7 °C)	255.3
17.04.2012 (15:05)	61.3	88.6	218 (26.0 °C)	26 (26.7 °C)	6.69 (24.2 °C)	1.1774 (23.5 °C)	250.7
17.04.2012 (16:00)	67.0	108.3	217 (26.8 °C)	19 (27.7 °C)	6.68 (25.1 °C)	1.1771 (23.5 °C)	252.2
17.04.2012 (17:45)	75.1	144.9	216 (26.1 °C)	-1 (27.4 °C)	6.85 (24.7 °C)	1.1722 (23.9 °C)	241.8
17.04.2012 (19:30)	80.5	180.1	219 (26.6 °C)	19 (27.6 °C)	6.71 (24.3 °C)	1.1782 (23.8 °C)	254.2
17.04.2012 (21:40)	84.2	222.0	219 (26.5 °C)	9 (26.2 °C)	6.67 (24.1 °C)	1.1779 (23.6 °C)	252.7
18.04.2012 (03:35)	91.4	332.8	217 (27.7 °C)	38 (27.7 °C)	6.69 (23.4 °C)	1.1781 (23.6 °C)	251.8
18.04.2012 (12:55)	94.5	496.5	219 (26.5 °C)	42 (26.3 °C)	6.65 (23.5 °C)	1.1779 (23.3 °C)	251.6
19.04.2012 (10:55)	96.7	851.9	221 (23.0 °C)	32 (23.0 °C)	6.69 (20.5 °C)	1.1794 (20.5 °C)	251.4
20.04.2012 (11:25)	100.2	1,260.4	216 (26.6 °C)	27 (26.2 °C)	6.77 (26.5 °C)	1.1791 (23.1 °C)	267.2
23.04.2012 (13:05)	98.6	2,354.4	215 (26.6 °C)	46 (26.6 °C)	6.77 (26.6 °C)	1.1798 (23.6 °C)	261.4

Temperature at measurement is shown in brackets

σ electric conductivity; ρ density; TDS total dissolved solids

Fig. 6 Changes of density (circles) and TDS (squares) during plant operation in April 2012. Onsite determinations at ambient pressure and temperature. Temperature development at the well head is shown as dashed line



and chloride for 0.5 M (Fig. 11a). Other elements, such as iron, showed rather unstable concentrations (between 1.1 and 2 mM) at cooler temperatures in 2011 and stabilized later with increasing temperatures until a constant value of about 1.2 mM was established during the course of measurements in 2012 (Fig. 11b).

Comparison of physicochemical data recorded by FluMo with data measured in simultaneously collected samples

Results obtained by FluMo show fluctuations of all measured physicochemical parameters at the beginning of the plant operation. This effect is mainly caused due to strong

changes of surface fluid temperature or thermodynamic disequilibrium. Data variability decreased after temperature stabilization in above-ground facility and relatively constant values for acidity, density, and redox potential established indicating the fluid to be in chemical equilibrium.

The comparison of in situ (FluMo) measured parameters (density, Eh and pH) with onsite determinations in collected samples cooled down to room temperature before measurement shows little differences (Fig. 12). It was found that all parameters show greater values when measured at ambient conditions. This difference increases with increasing fluid temperature in the plant, indicating that chemical reactions such as mineral precipitation occur

Fig. 7 Redox (*circles*) and pH-values (*shift-corrected; squares*) during the 7-day production test. Onsite determination at ambient pressure and temperature. Temperature development at the well head is shown as *dashed line*

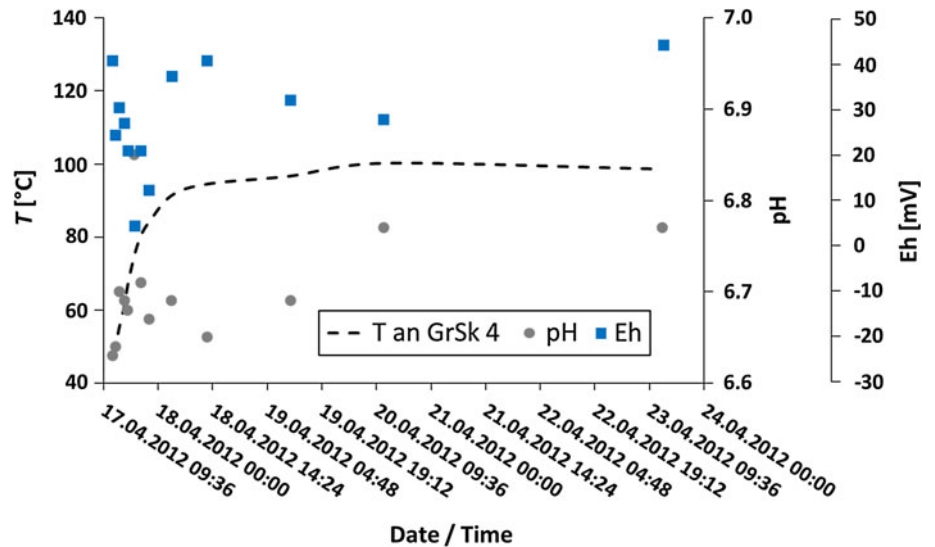


Fig. 8 Variation of temperature, electrical conductivity, total organic carbon (TOC), and TDS in GrSk-fluid during continuous operation (17–24 April 2012)

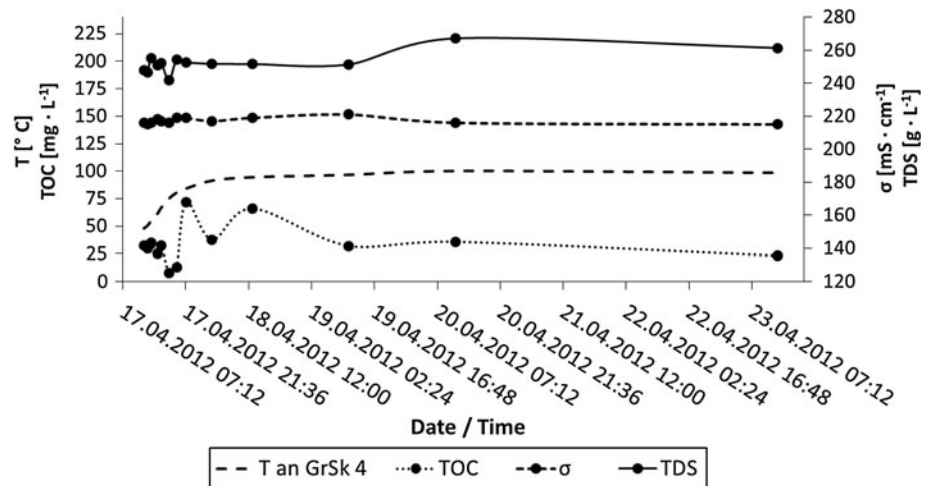
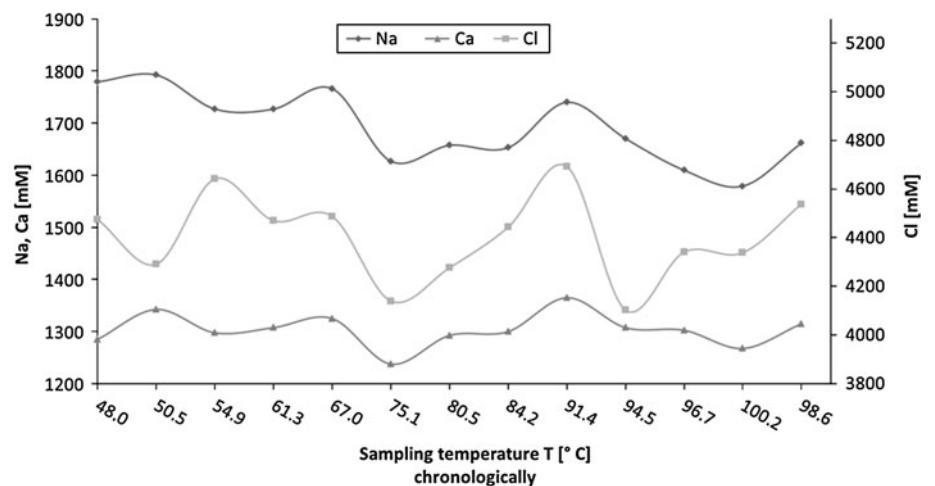


Fig. 9 Concentration of dissolved main components (Na, Ca, Cl) of the GrSk fluid in dependence on the temperature during continuous 7-day operation (April 2012)



during fluid cooling (Fig. 12). Elevated pH values could also be explained by CO₂ degassing, but since the CO₂ content of the fluid is relatively low (<0.1 Vol.%), the

degassing effect can only be of minor impact. In general, the pH values of both measurement techniques are roughly in the same order of magnitude and the trends correlate

Fig. 10 Concentration of dissolved minor components (Fe, Mn, Si, Zn, Ba, Pb) of the GrSk fluid in dependence on the temperature during continuous 7 day operation (April 2012)

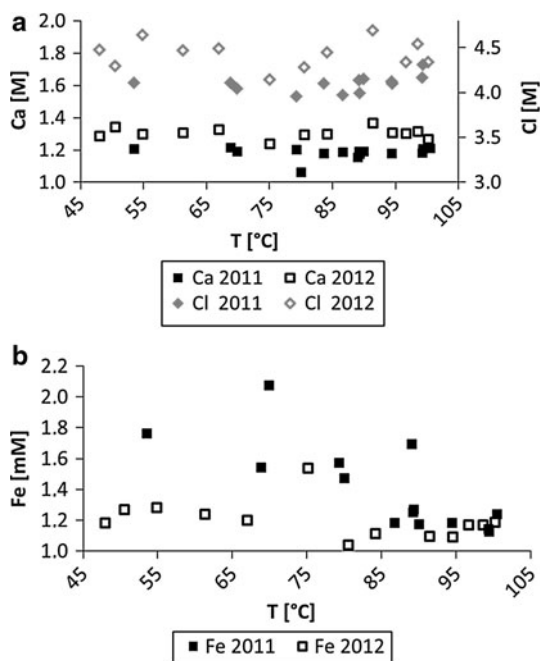
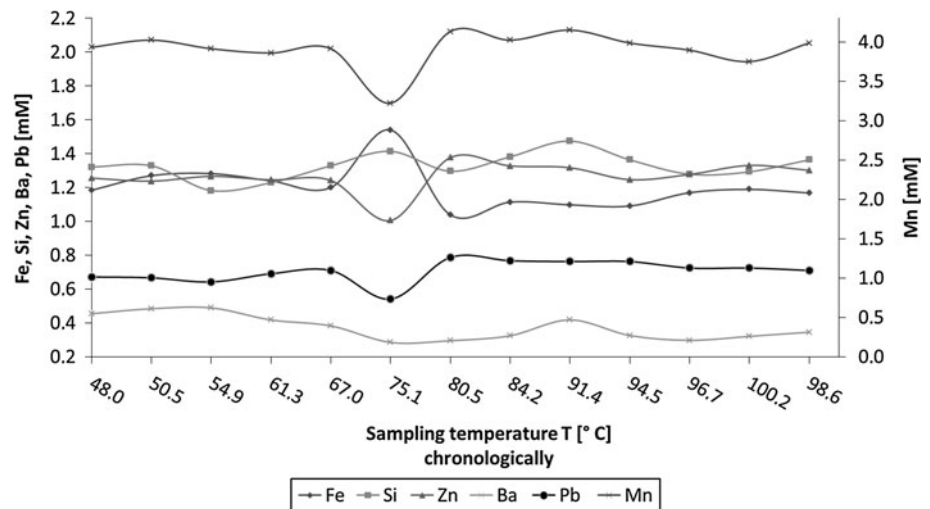


Fig. 11 Comparison of analytical results from August/September 2011 with April 2012. Concentration development of calcium and chloride (a) and iron (b) in dependence of fluid temperature

quite well. Significant differences in redox values can be attributed to the strong effect of temperature on the Eh value according to the Nernst equation (samples collected at high T were cooled down to room temperature before measurements).

Conclusion and outlook

This study revealed that the application of FluMo for online measurements under in situ conditions provides highly accurate time-resolved data which clearly differ

from measurements of conventionally obtained data (by collecting samples, cooling them down and measuring). This implies also that physicochemical data, described in former studies, have to be considered with caution considering the fact that usually fluids are cooled down before measurements. FluMo definitely provides more realistic results of physicochemical properties of the fluid.

Mainly at the beginning of the plant operation irregularities of pH-, Eh value, and density have been observed both at in situ and onsite measurements. They can be explained by several processes: One possibility could be that chemical reactions are taking place in the borehole of the production well. It has been observed from gas measurements that during downtime of the pumps high hydrogen concentration (up to 8 Vol.%) appeared in the gas phase. Hydrogen is an indicator of steel corrosion and it is also a strong reducing agent which could thus be responsible for further redox reactions and changes in redox and pH- conditions. However, this does not explain density changes. Therefore, another explanation for fluctuations in chemical composition (including density) could be the presence of crude oil in the reservoir fluid which appears at irregular intervals at the borehole. Finally, it could be possible that different ratios of mixed fluid from different layers of the reservoir enter the borehole. Altogether, three layers (one vulcanite and two sandstone formations with different content of conglomerate and clay) have been hydraulically stimulated. The perforation of the production well has enabled access to the reservoir at different depths: 4118–4122; 4204–4208 m MD (Zimmermann and Reinicke 2010). However, further investigation of fluid composition, e.g. isotope ratios have to be measured to confirm that hypothesis.

Although FluMo obtained very good results in the present study, it has to be emphasized that at highly saline and high-temperature conditions the internal reference

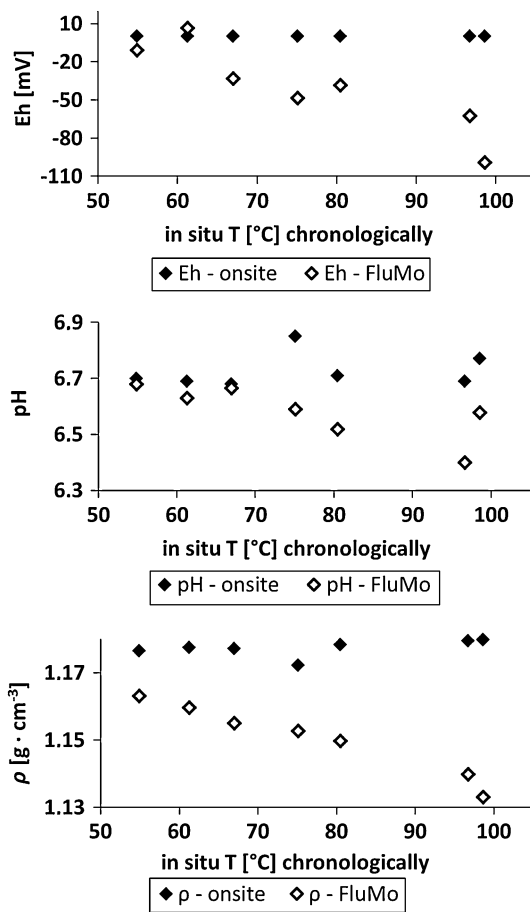


Fig. 12 Comparison of Eh- (*top*), pH (*middle*), and density (*bottom*) data of in situ measurements with FluMo and of onsite measurements in collected samples cooled down to room temperature

system of pH- and redox electrodes easily becomes contaminated with the various fluid components. In addition, quick precipitation (e.g. of barite) from the saturated thermal water on membranes and diaphragms of all probes causes damages or errors in measurements and reduces the lifetime of the electrodes.

Experiments with FluMo are not yet terminated. Apart from testing different types of potentially more resistant electrodes, also the integrated heat exchanger needs to be tested. An initial test during the experimental week in April 2012 already revealed good functionality (Milsch et al. 2013).

The ultimate goal of the application of FluMo will be to measure permanently during fluid production the physico-chemical parameters to obtain long-term results on reservoir development. Experiments from the heat exchanger will deliver additional information on temperature effect and kinetic of scale formation within the geothermal plant.

Acknowledgments The authors gratefully thank the FluMo development group Ronny Giese, Mathias Poser, and Stefan Kranz. They

also acknowledge Alexandra Vetter, Andrea Vieth-Hillebrand, Kristin Günther, Andreas Kratz, Rudolf Naumann, and the staff of the VKTA Laboratory for their technical and analytical support. Special thanks also to the Technical Support Service of Endress + Hauser Messtechnik and of Emerson Process Management. Financial support from the federal ministry of environment (BMU) and the ministry of research and education (BMBF) is gratefully acknowledged.

References

Altmairer M, Metz V, Neck V, Müller R, Fanghänel TH (2003) Solid-liquid equilibria of Mg(OH)₂(cr) and Mg₂(OH)₃Cl₄H₂O(cr) in the system Mg–Na–H–OH–Cl–H₂O at 25 °C. *Geochim Cosmochim Acta* 67(19):3595–3601. doi:10.1016/S0016-7037(03)00165-0

Blöcher G, Moeck I, Milsch H, Zimmermann G (2008) Modelling of pore pressure response due to hydraulic stimulation treatments at the geothermal research doublet EGRSK3/90 and GTGRSK4/05 in summer 2007. In: proceedings of the 33rd workshop on geothermal reservoir engineering Stanford USA 2008

Buffe J, Horvai G (eds) (2000) In situ monitoring of aquatic systems: chemical analysis and speciation. Wiley-VCH, Weinheim, pp 13–20

Bührke T, Wengenmayr R (2012) Erneuerbare Energie. Alternative Energiekonzepte für die Zukunft. In: Huenges E (ed) Geothermische Wärme- und Stromerzeugung. Energie aus der Tiefe. Wiley-VCH, Weinheim, pp 52–58

Bukatsch F (1938) Die Wirkung von Radon und von Mineralstoffen auf die Photosynthese der Sabmersen. Ein Beitrag zur Erklärung des Einflusses von Gasteiner Thermalwasser auf die Kohlensäureassimilation von Wasserpflanzen. *Planta* 28(2):264–274. doi:10.1007/BF01909523

Eggeling L, Köbel T, Schlagermann P, Münch W (2011) Geothermische stromerzeugung in Deutschland. *Chem Ing Tech* 83(11):1834–1844. doi:10.1002/cite.201100089

Friberg L, Poelchau HS, Krooss B, Littke R (2000) 3D-modelling of thermal history and simulation of methane and nitrogen migration along the Northeast German seismic DEKORP profile 9601. *J Geochem Explor* 69–70:263–267

Gultekin F, Hatipoglu E, Ersoy AF (2011) Hydrogeochemistry, environmental isotopes and the origin of the Hamamayagi-Ladik thermal spring (Samsun, Turkey). *Environ Earth Sci* 62(2011):1351–1360. doi:10.1007/s12665-010-0621-4

Hall K, Niessner R (2010) Wasser: Nutzung im Kreislauf: Hygiene, Analyse und Bewertung. Walter de Gruyter, Berlin, p 163

Huenges E (2004) Energie aus der Tiefe: Geothermische Stromerzeugung. *Phys Unserer Zeit* 35(6):282–288. doi:10.1002/piuz.200401050

Huenges E (ed) (2010) Geothermal energy systems: exploration, development and utilization. Wiley-VCH, Weinheim, p 463

Huenges E, Trautwein U, Legarth B, Zimmermann G (2006) Fluid pressure variation in a sedimentary geothermal reservoir in the North German Basin: case study Groß Schönebeck. *Pure Appl Geophys* 163(10):2141–2152. doi:10.1007/s00024-006-0122-2

Kühn M (1997): Geochemische Folgereaktionen bei der hydrogeothermalen Energiegewinnung. *Berichte/Fachbereich Geowissenschaften, Universität Bremen* 92, 129

Liu Y, Zhou X, Fang B, Zhou H, Yamanaka T (2012) A preliminary analysis of the formation of travertine and travertine cones in the Jifei hot spring, Yunnan, China. *Environ Earth Sci* 66(2012):1887–1896. doi:10.1007/s12665-011-1413-1

Lüders V, Reutel C, Hoth P, Banks DA, Mingram B, Pettke T (2005) Fluid and gas migration in the North German Basin: fluid inclusion and stable isotope constraints. *Int J Earth Sci*

- (GeolRundsch) 94(5–6):990–1009. doi:[10.1007/s00531-005-0013-2](https://doi.org/10.1007/s00531-005-0013-2)
- Lüders V, Plessen B, Romer RL, Weise SM, Banks DA, Hoth P, Dulski P, Schettler G (2010) Chemistry and isotopic composition of Rotliegend and Upper Carboniferous formation waters from the North German Basin. *Chem Geol* 276(2010):198–208. doi:[10.1016/j.chemgeo.2010.06.006](https://doi.org/10.1016/j.chemgeo.2010.06.006)
- Magri F, Bayer U, Jahnke C, Clausnitzer V, Diersch HJ, Fuhrman J, Möller P, Pekdeger A, Tesmer M, Voigt HJ (2005) Fluid-dynamics driving saline water in the North East German Basin. *Int J Earth Sci* 94(5–6):1056–1069. doi:[10.1007/s00531-005-0497-9](https://doi.org/10.1007/s00531-005-0497-9)
- Milsch H, Giese R, Poser M, Kranz S, Feldbusch E, Regenspurg S (2013) FluMo—A mobile fluid-chemical monitoring unit for geothermal plants. *Environ Earth Sci* (this issue)
- Norden B, Förster A, Balling N (2008) Heat flow and lithospheric thermal regime in the Northeast German Basin. *Tectonophysics* 460(1–4):215–229. doi:[10.1016/j.tecto.2008.08.022](https://doi.org/10.1016/j.tecto.2008.08.022)
- Regenspurg S, Wiersberg T, Brandt W, Huenges E, Saadat A, Schmidt K, Zimmermann G (2010) Geochemical properties of saline geothermal fluids from the in situ geothermal laboratory Groß Schönebeck (Germany). *Chem Erde* 70(3):3–12. doi:[10.1016/j.chemer.2010.05.002](https://doi.org/10.1016/j.chemer.2010.05.002)
- Scheck M, Bayer U (1999) Evolution of the Northeast German Basin—inferences from a 3D structural model and subsidence analysis. *Tectonophysics* 313(1–2):145–169
- Schmidt Mumm A, Wolfgramm M (2002) Diagenesis and uid mobilisation during the evolution of the North German Basin—evidence from fluid inclusion and sulphur isotope analysis. *Mar Pet Geol* 19(3):229–246
- Schmidt Mumm A, Wolfgramm M (2004) Fluid systems and mineralization in the North German and Polish Basin. *Geofluids* 4(4):315–328. doi:[10.1111/j.1468-8123.2004.00090.x](https://doi.org/10.1111/j.1468-8123.2004.00090.x)
- Tenzer H, Park C-H, Kolditz O, McDermott CI (2010) Application of the geomechanical facies approach and comparison of exploration and evaluation methods used at Soultz-sous-Forêts (France) and Spa Urach (Germany) geothermal sites. *Environ Earth Sci* 61(2010):853–880. doi:[10.1007/s12665-009-0403-z](https://doi.org/10.1007/s12665-009-0403-z)
- Tesmer M, Möller P, Wieland P, Jahnke C, Voigt H, Pekdeger A (2007) Deep reaching fluid flow in the North East German Basin: origin and processes of groundwater salinisation. *Hydrogeol J* 15(7):1291–1306. doi:[10.1007/s10040-007-0176-y](https://doi.org/10.1007/s10040-007-0176-y)
- Zimmermann G, Reinicke A (2010) Hydraulic stimulation of a deep sandstone reservoir to develop an enhanced geothermal system: laboratory and field experiments. *Geothermics* 39(1):70–77. doi:[10.1016/j.geothermics.2009.12.003](https://doi.org/10.1016/j.geothermics.2009.12.003)